

EXPERIMENTAL RESEARCH REGARDING TRANSIENT REGIME OF KINEMATIC CHAINS INCLUDING PLANETARY TRANSMISSIONS USED IN INDUSTRIAL ROBOTS

Butunoi Paul-Alin¹, Stan Gheorghe²

^{1, 2} "Vasile Alecsandri" University of Bacau, "Department of Industrial Engineering
Calea Marasesti Street, No. 157, 600115 Bacau, Romania

Corresponding author: Butunoi Paul-Alin, alin.butunoi@gmail.com

Abstract: It is very important to know the transient regimes of kinematic chains used for positioning in the industrial robots as well as the factors of influence. Therefore, a good transient regime leads to both low response times and path error, the latter being compared to the imposed path. In this paper, an experimental approach concerning the transient regimes is proposed. The kinematic chain being investigated, includes a two-stage planetary transmission type ANGRED 2P12, having a reduction ratio of $i=37.7$. Experimental research was done with a Renishaw ML10 interferometer, using as variable parameters, speed and load respectively. The reduction ratio of the planetary gear has, on the other side, a greater influence over the response times and path error, as the speed of the moving element increases. Therefore, some optimization strategies concerning the reduction ratio can be made based on the results obtained during the experimental research.

Key words: gear ratio, interferometer, response times, guideway, variable frequency drive.

1. INTRODUCTION

The transient regime itself has a very significant importance over the positioning accuracy of the industrial robot, since the path error is influenced by the response times during the acceleration and braking of the kinematic chain (Stan, 1999), (Antonovics, 2009). If we study the movement of the aforementioned kinematic chain, from its starting and stopping time, we will identify three main phases, shown in Fig. 1 (: the starting phase, the regime phase and the stopping (or braking) phase.

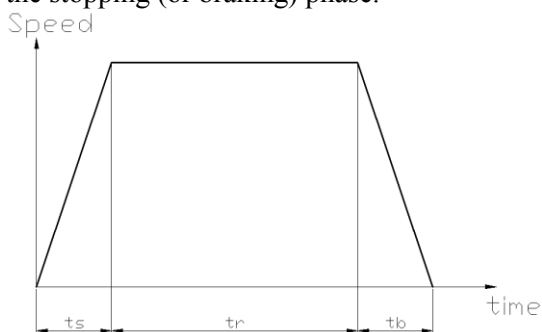


Fig. 1. Theoretical diagram of the transient regime (Stan, 2009)

During the starting phase, the movement speed of the robot arm continuously increases until it reaches a certain value named regime (or working) speed. During the regime phase, the speed is considered to be constant. However, there are some oscillations around the value of the regime speed. The braking phase represents in fact, the opposite of the starting phase, the speed of the robot arm decreases until it reaches zero. It is obvious the fact that, for each of the three phases previously described, it corresponds three response times: the starting time (t_s), the regime time (t_r) and the braking time (t_b). The sum between these times represents the total time, denoted t_t . According to the standard ISO 9283, the effective (or attained) transient regime differs from the theoretical one, shown in figure 1, by the corner error and speed precision on the imposed trajectory. A theoretical study concerning the optimization of the response times by optimizing the shape of the planet carrier of a planetary speed reducer is proposed by (Butunoi, 2013). In this paper, an experimental approach is used in order to determine the transient regimes of a kinematic chain including a two-stage planetary transmission, ANGRED 2P12 type, having a gear ratio $i=37.7$. The experiments were done at constant speed and load respectively, using a Renishaw ML10 laser interferometer. Based on the obtained results, some optimization strategies concerning the response times can be proposed.

2. DESCRIPTION OF THE EXPERIMENTAL SETUP AND THE PLANETARY TRANSMISSION USED

The designed experimental testing rig is shown in Fig. 2 along with the principle diagram shown in Fig. 3. The electric motor that drives the input shaft of the two-stage planetary transmission has the nominal power of 1.5kW. On the planetary transmission's output shaft, a roller 1 (having a radius R_1) is attached, driving the roller 2 (having a radius R_2) using a wire 3, with a 2mm diameter. With this resulting wire transmission, the

moving element 4 executes the translation movement denoted by I in Figure 3, along the guidance rail 5, forming therefore a rolling guideway. Since $R_1=R_2$, the

angular speeds of these two will be equal ($\omega_1=\omega_2$), the transmission ratio between the rollers being equal to unity.

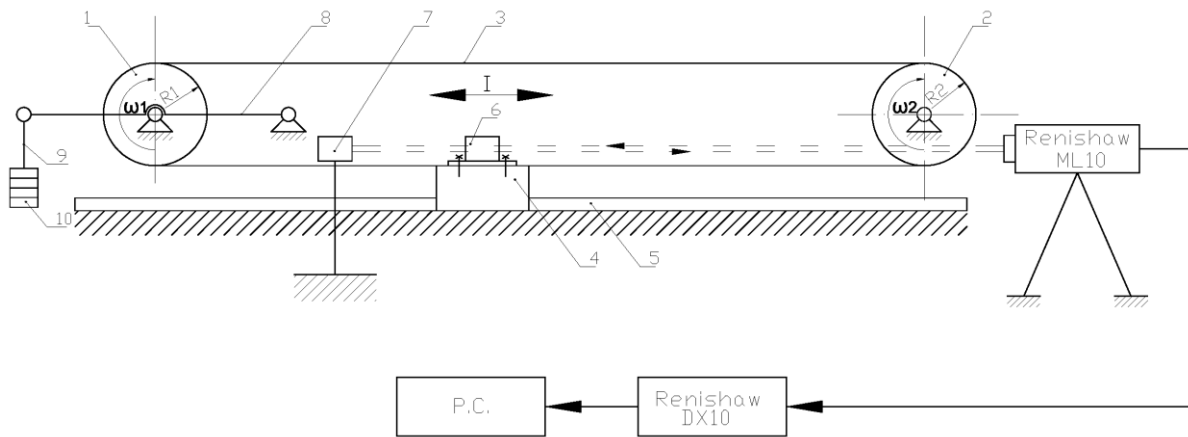


Fig. 2. Schematic diagram of the used measuring principle for transient regimes (1 –driving roller, 2 – driven roller, 3 – wire, 4 – moving element, 5 – guidance rail, 6 – moving optical prism, 7 – stationary optical prism, 8 – brake arm, 9 – rod, 10 – weights)

A rolling guideway was chosen thanks to its lower friction between the moving element 4 and rail 5, compared to a sliding guideway, therefore reducing the effort necessary to drive the moving element 4. On the moving element 4, the optical prism 6 is attached, moving in relation to the stationary optical prism 7. The laser signal is given and taken back by the laser source type Renishaw ML10 and converted to a numerical signal, sent through the DX10 interface to a computer. This measuring assembly is also known as interferometer assembly. The braking system attached to the planetary transmission's output shaft, allows the adjustment of the load, during the experiments. The

braking system is composed of the brake arm 8, at its end being attached the rod 9 on which weights 10 are added. Values for the load, used during the experiments are: 0 (idle); 2.2; 4.4; 6.6; 8.8, 12.1 and 15.4 [kgf]. The adjustment of the electric motor speed is done, using a variable frequency drive (VFD), type Altivar 58, manufactured by the Schneider Electric company. Values for the frequencies used during the experiments are: 2; 10; 20; 30; 40; 50 and 60 [Hz]. In order to make a correlation between the speeds of the electric motor and the values given above for the frequencies set from the Altivar 58 variable frequency drive, the diagram presented in Fig. 3 is given.

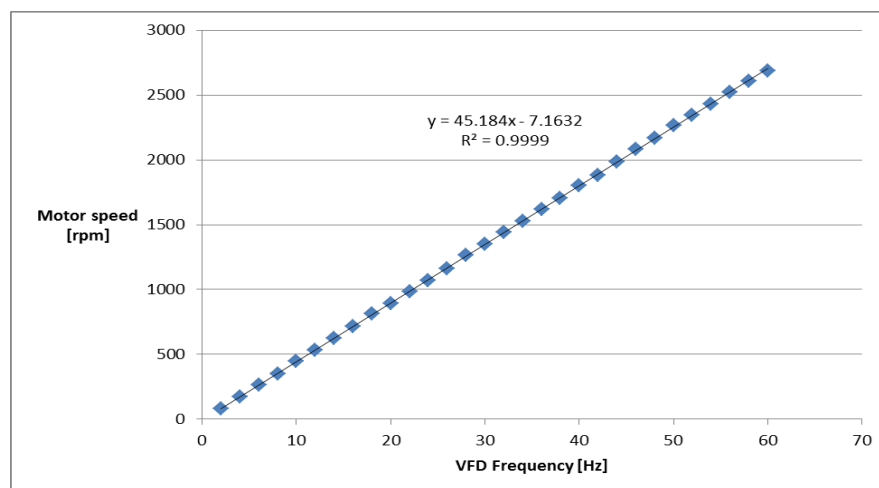


Fig. 3. Correlation diagram showing the link between the frequency set from the VFD and motor speed

A sectional view of the planetary transmission used for the experimental research, is given in Fig. 4, along with the kinematic diagram shown in Fig. 5. Concerning this planetary transmission, an angular profile shifting of the sun and planet gears corresponding to the second stage was done, in order to minimize the flank play to an imposed value of 0.02mm. The second stage was

chosen because the flank and angular plays of the first stage are reduced by the corresponding ratio ($i=6.14$) and also, the peripheral speeds of the gears and planet carrier corresponding to the second stage have lower values, therefore a small influence over the thermal regime of the planetary speed reducer.

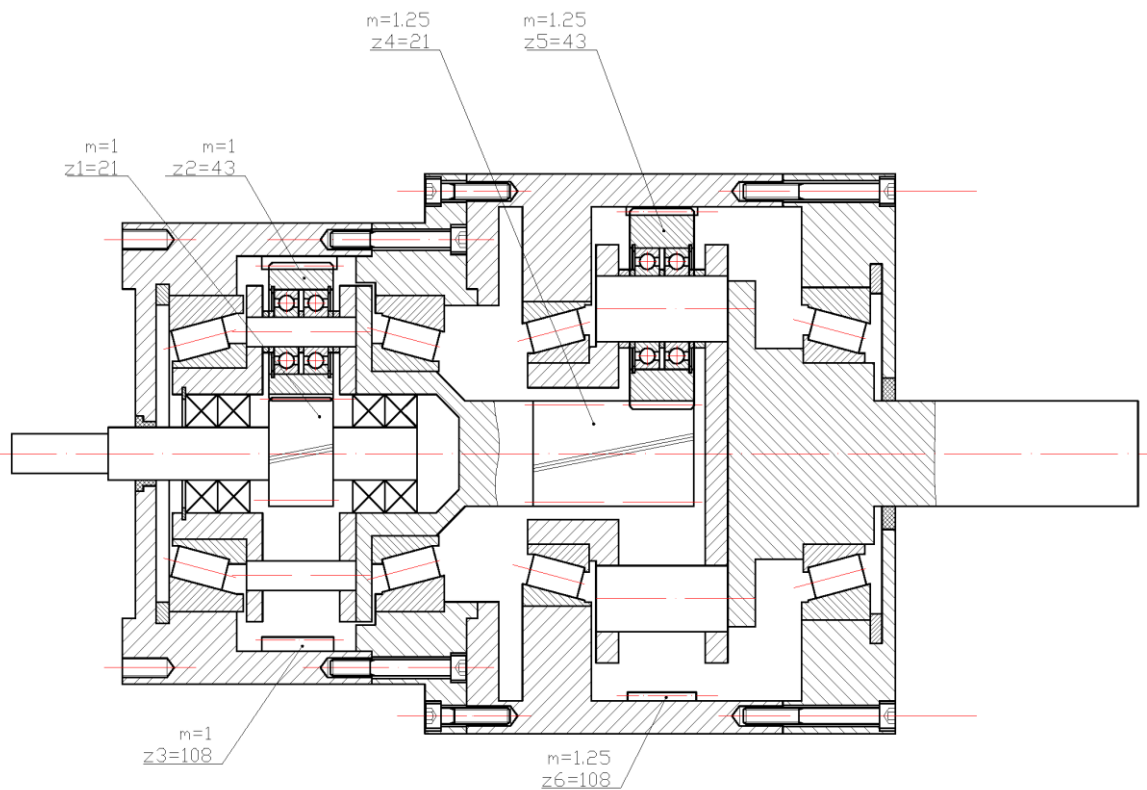


Fig. 4. Sectional drawing of the two-stage ANGRED 2P12 planetary transmission

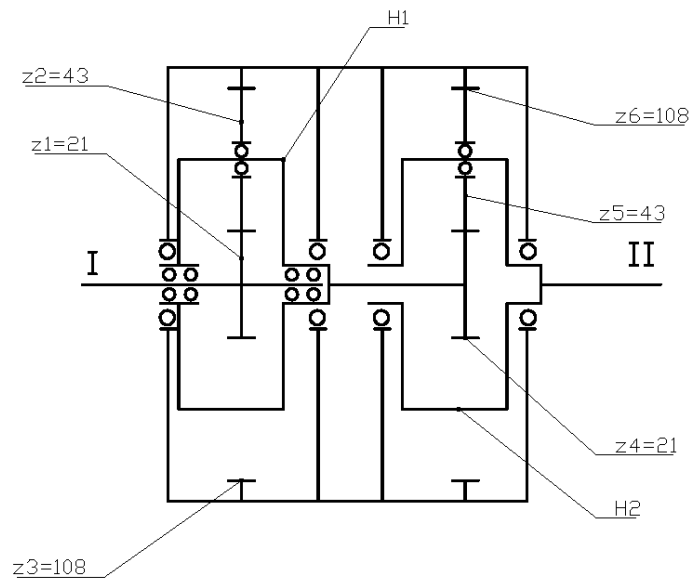


Fig. 5. Kinematic diagram of the two-stage ANGRED 2P12 planetary transmission

Analysing the sectional drawing shown in Fig. 4, reveals that the planetary transmission used during the experiments has a good degree of stiffness. It can be noted that the bearings that support both planet carriers (denoted by H_1 and H_2) in the kinematic diagram presented in figure 5, are disposed in the “O” shape. According to the kinematic diagram shown in Fig. 5, the input element of the first stage represents the sun gear z_1 attached to the shaft I, while the output element represents the planet carrier H_1 . Similarly, for the second stage, the input element is given by the sun gear z_4 , while

the output element is given by the planet carrier H_2 , attached to the shaft II. Also, using the method described by (Gafitanu, 2009) and (Stan, 1999), the bearing preload was optimized in order to improve their stiffness. Moreover, the applying of the optimized pretensioning load avoids the operation of the bearing in the area of higher deformations. The overall efficiency of the planetary transmission was also improved by using NanoLub transmission oil additive with fullerene WS_2 (Ratoi et. al., 2006). Applying these improvement strategies, a “new” planetary speed reducer resulted,

which was used for conducting the experimental research presented in this paper. These optimization strategies were necessary so that the planetary transmission used fulfills the requirements for the gear transmissions used in industrial robots.

3. RESULTS AND DISCUSSIONS

A graphical representation concerning the transient regimes, characterized by the parameters given in Table 1, Table 2, Table 3, Table 4, Table 5, Table 6 as well as Table 7, are given in Fig. 6 and Fig. 7 respectively. The transient regime shown in Fig. 6 corresponds to the lowest frequency set from the variable frequency drive, while the graphical representation shown in Fig. 7, represents a comparison between the transient regimes, corresponding to the frequencies of 10, 20, 30, 40, 50 and 60Hz (starting from bottom to top). Analysing the graphical representations as well as the numerical

results shown in Tables 1 to 7, it is revealed that, the speed of the moving element increases with the frequency set from the variable frequency drive (basically the speed of the electric motor). Of course, by increasing the speed of the moving element, the distance travelled decreases, as well as the total time (t_t). However, it is recorded an increase concerning the starting and braking times. This is due to the inertia of the gears and carrier forming the planetary transmission, as well as the inertia of the electric motor or moving element. Also, the gear ratio of the planetary transmission has an influence concerning the overall transient regime. The influence of the planetary transmission's reduction ratio becomes significant, as the speed of the moving element increases. Therefore, some optimization strategies that concern the link between the planetary transmission's reduction ratio, the motor and load inertia can be made.

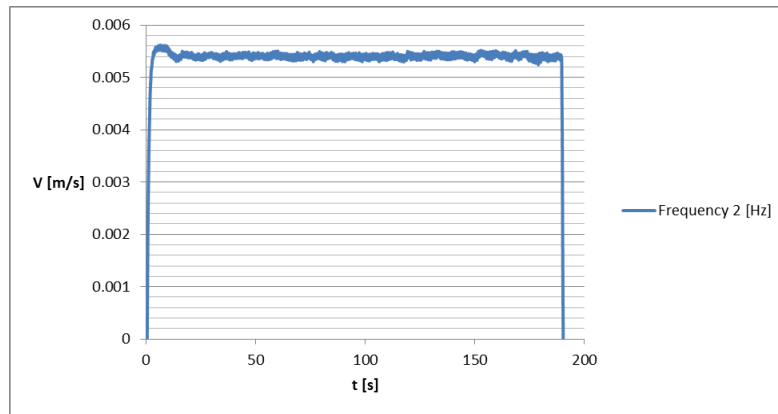


Fig. 6. The transient regime corresponding to the frequency of 2 [Hz]

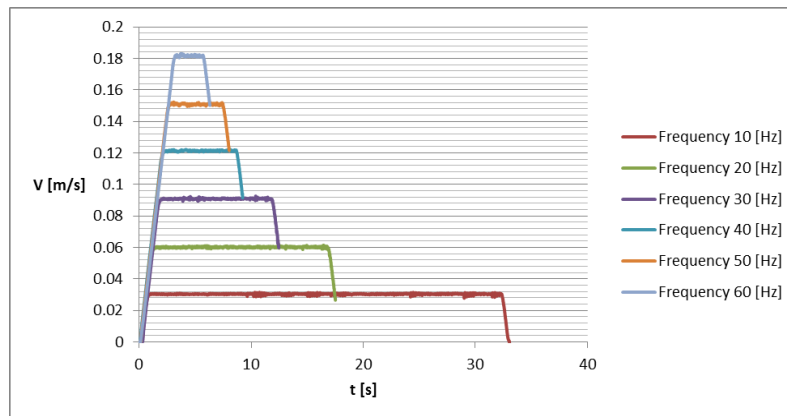


Fig. 7. The transient regime corresponding to the frequencies of 10, 20, 30, 40, 50, 60 [Hz] (at constant load)

Numerical results concerning the parameters of the transient regime (response times and speed of the moving element) are given in Tables 1, to 7 (for the values given in this paper corresponding to load and frequency set from the variable frequency drive). It can be noticed that, by increasing the load value at the output shaft, a corresponding increase of the starting time (t_s) can be noticed, while the braking time (t_b)

decreases. Therefore, the value of the regime time (t_r) and total time (t_t) modifies accordingly. Concerning the speed of the moving element 4, it shows a decrease in value, as the load increases, as a result of the increase concerning the friction torque (resistant torque) at the planetary transmission's output shaft. According to Fig. 6, and Fig. 7 as well as the numerical data shown in the tables, the minimum positioning time, depends on the

distance travelled by the robotic arm. Also, according to the ISO 9283 standard, the positioning times (or response times) contribute to the total time, as shown by the experimental results.

Concerning the results presented in graphical form, it can be noticed that the corner error, speed precision,

fluctuation and repeatability, parameters that are defined by the ISO 9283 standard, reside between acceptable limits, based on the graphical results, the fluctuations encountered being minimal.

Table 1. Parameters of the transient regime during idle operation

VFD Frequency [Hz]	t_s [s]	t_r [s]	t_b [s]	t_t [s]	V [$m \cdot s^{-1}$]
2	0.68	187.94	0.68	189.3	0.0054
10	0.84	31.204	0.837	32.881	0.0301
20	1.032	15.596	1.01	17.638	0.06
30	1.67	9.548	1.428	12.646	0.091
40	2.052	6.72	2.044	10.816	0.120
50	2.534	4.976	2.648	10.158	0.151
60	3.044	2.912	2.848	8.804	0.181

Table 2. Parameters of the transient regime during operation at 2.2 [kgf]

VFD Frequency [Hz]	t_s [s]	t_r [s]	t_b [s]	t_t [s]	V [$m \cdot s^{-1}$]
2	0.658	191.61	0.657	192.92	0.0054
10	0.674	32.636	0.66	33.97	0.0318
20	1.122	15.556	1	17.678	0.06
30	1.498	9.716	1.732	12.946	0.084
40	2.094	6.264	2.118	10.476	0.12
50	2.668	4.84	2.486	9.994	0.152
60	2.74	2.736	2.9	8.376	0.1804

Table 3. Parameters of the transient regime during operation at 4.4 [kgf]

VFD Frequency [Hz]	t_s [s]	t_r [s]	t_b [s]	t_t [s]	V [$m \cdot s^{-1}$]
2	0.396	189.6	0.236	190.23	0.0055
10	0.954	33.6	0.726	35.284	0.03
20	1.064	15.24	1.16	17.464	0.06
30	1.58	9.676	1.396	12.652	0.084
40	2.288	6.324	2.12	10.732	0.12
50	2.416	4.948	2.524	9.888	0.151
60	2.808	3.092	2.948	8.848	0.18

Table 4. Parameters of the transient regime during operation at 6.6 [kgf]

VFD Frequency [Hz]	t_s [s]	t_r [s]	t_b [s]	t_t [s]	V [$m \cdot s^{-1}$]
2	0.396	194.1	0.492	195	0.0054
10	0.88	34.368	0.876	36.12	0.03
20	1.064	15.94	1.15	18.15	0.06
30	1.58	9.376	1.58	12.53	0.084
40	2.104	6.512	2.144	10.76	0.122
50	2.692	4.496	2.844	10.03	0.15
60	3.256	3.104	3.006	9.36	0.181

Table 5. Parameters of the transient regime during operation at 8.8 [kgf]

VFD Frequency [Hz]	t_s [s]	t_r [s]	t_b [s]	t_t [s]	V [$m \cdot s^{-1}$]
2	0.464	197.0	0.404	197.8	0.005
10	0.902	32.61	0.572	34.08	0.03
20	0.932	15.85	1.023	17.80	0.06
30	1.546	10.28	1.624	13.45	0.091
40	2.062	6.572	2.144	10.77	0.12
50	2.544	5.024	2.61	10.17	0.148
60	3.2	3.08	3.164	9.444	0.179

Table 6. Parameters of the transient regime during operation at 12.1 [kgf]

VFD Frequency [Hz]	t_s [s]	t_r [s]	t_b [s]	t_t [s]	V [m·s ⁻¹]
2	0.514	195.9	0.35	196.7	0.0054
10	0.684	36.43	0.52	37.64	0.0291
20	0.966	16.6	0.95	18.52	0.062
30	1.43	9.36	1.63	12.42	0.09
40	1.808	6.348	1.94	10.1	0.12
50	2.364	4.9	2.36	9.628	0.15
60	2.816	2.952	2.94	8.708	0.181

Table 7. Parameters of the transient regime during operation at 15.4 [kgf]

VFD Frequency [Hz]	t_s [s]	t_r [s]	t_b [s]	t_t [s]	V [m·s ⁻¹]
2	0.77	195.676	0.418	196.864	0.0054
10	0.846	34.92	0.441	36.207	0.0294
20	1.008	16.83	0.9	18.738	0.06
30	1.448	10.176	1.428	13.052	0.09
40	1.972	7.228	1.892	11.092	0.12
50	2.586	4.824	2.232	9.642	0.15
60	3.03	2.752	2.86	8.642	0.181

Concerning the results presented in graphical form, it can be noticed that the corner error, speed precision, fluctuation and repeatability, parameters that are defined by the ISO 9283 standard, reside between acceptable limits, based on the graphical results, the fluctuations encountered being minimal.

4. CONCLUSIONS

In this paper, an experimental approach was proposed, in order to determine the parameters of the transient regime of a kinematic chain that includes a two-stage planetary transmission. The testing rig was presented, along with the results obtained (presented in tabular and graphical form). The results show the importance of the transient regime itself over the path error corresponding to the positioning kinematic chains of the industrial robots. The planetary transmission's ratio, inertia and efficiency are the basic parameters that influence the performance of the overall kinematic chain. The structure of the industrial robot is therefore necessary to be established by the manufacturer, starting from the perspective of achieving minimum inertias and response times for its controlled axes, respectively. Also, the experimental research concerning the transient regime, done using as influencing factors the speed of the electric motor driving the planetary transmission (set using the variable frequency drive) and the load applied at the input shaft, allows the manufacturers of industrial robots and planetary transmissions to choose the best solution concerning the increase of performances of their products.

5. REFERENCES

1. Antonovics U, Brazis V, Greivulis J (2009), *The Mechanical Transient Process at Asynchronous Motor Oscillating Mode*, Sci. Proc. of Riga Technical University, pp 23-26.
2. Butunoi P A, Stan G, Ciofu C (2013), *Research regarding improvement of dynamic behaviour for high-ratio planetary gears*. Appl. Mech. and Materials, 657 pp. 549-553.
3. Gafitanu M., (1983) *Machine Elements*. Vol. 2, Technical Publishing House Bucharest.
4. Ratoi M., Niste V. B., Zekonyte J. (2014) *WS₂ Nanoparticles – Potential Replacement for ZDDP and Friction Modifier Additives* in 19th International Colloquium Tribology.
5. Stan G., (2009) *Closed-Loop Mechanical Transmissions*, Iasi Junimea Publishing House, Iasi pp. 148-190.
6. *** ISO 9283: *Manipulating Industrial Robots - Performance Criteria and Related Test Methods*.

Received: January 15, 2016 / Accepted: June 10, 2016 / Paper available online: June 20, 2016 © International Journal of Modern Manufacturing Technologies.